

ONCOGENOMICS

Comparative expression profiling identifies an *in vivo* target gene signature with TFAP2B as a mediator of the survival function of PAX3/FKHR

M Ebauer, M Wachtel, FK Niggli and BW Schäfer

Department of Oncology, University Children's Hospital, Zurich, Switzerland

The chromosomal translocation t(2;13), characteristic for the aggressive childhood cancer alveolar rhabdomyosarcoma (aRMS), generates the chimeric transcription factor PAX3/FKHR with a well known oncogenic role. However, the molecular mechanisms mediating essential pathophysiological functions remain poorly defined. Here, we used comparative expression profiling of PAX3/FKHR silencing *in vitro* and PAX3/FKHR-specific gene signatures *in vivo* to identify physiologically important target genes. Hereby, 51 activated genes, both novel and known, were identified. We also found repression of skeletal muscle-specific genes suggesting that PAX3/FKHR blocks further differentiation of aRMS cells. Importantly, TFAP2B was validated as direct target gene mediating the anti-apoptotic function of PAX3/FKHR. Hence, we developed a pathophysiologically relevant transcriptional profile of PAX3/FKHR and identified a critical target gene for aRMS development.

Oncogene advance online publication, 21 May 2007; doi:10.1038/sj.onc.1210525

Keywords: alveolar RMS; chimeric transcription factor; expression profiling; TFAP2B; PAX3/FKHR

Introduction

Rhabdomyosarcoma (RMS) is a common childhood soft tissue sarcoma associated with the skeletal muscle lineage. On the basis of histology, two main subgroups of RMS, embryonal rhabdomyosarcoma (eRMS) and alveolar rhabdomyosarcoma (aRMS), are distinguished. The majority of cases of the more aggressive aRMS are associated with one of two reciprocal translocations t(2;13)(q35;q14) or t(1;13)(p36;q14), generating intronic fusions of PAX3 (or PAX7) and FKHR, also known as FOXO1A (Galili *et al.*, 1993). The fusion proteins contain the two DNA-binding domains of PAX3 or PAX7, namely a paired and, a homeodomain and the transactivation domain derived from FKHR.

Earlier studies on PAX3/FKHR support an oncogenic role of this fusion protein in tumor-initiation and maintenance. A tumor initiating effect has been evaluated *in vitro* where ectopic expression of PAX3/FKHR leads to transformation of chicken embryo fibroblast (Scheidler *et al.*, 1996), NIH3T3 cells (Lam *et al.*, 1999) and a human eRMS cell line (Anderson *et al.*, 2001). Furthermore, PAX3/FKHR induces murine aRMS postnatally in cooperation with other oncogenic events such as loss of Ink4A/ARF locus (Keller *et al.*, 2004). Involvement in tumor maintenance is reflected by the fact that downregulation of fusion protein activity by antisense oligonucleotides induces apoptosis (Bernasconi *et al.*, 1996). Similarly, an inducible transcriptional repressor induced tumor regression *in vivo* via extensive apoptosis (Ayyanathan *et al.*, 2000), suggesting that established RMS tumors are dependent on PAX3/FKHR expression.

At the molecular level, PAX3/FKHR is a stronger transactivator compared to wild-type PAX3 (Bennicelli *et al.*, 1995; Fredericks *et al.*, 1995). Therefore, the oncogenic properties of PAX3/FKHR are thought to base on dysregulation (that is upregulation or downregulation) of PAX3 target genes. However, recent studies suggested that PAX3/FKHR might alter the expression of gene targets quantitatively and qualitatively distinct from PAX3 (Epstein *et al.*, 1998; Begum *et al.*, 2005). Understanding the oncogenic function of PAX3/FKHR hence requires identification of the pathophysiologically relevant target genes. One difficulty in this search has been that most studies relied on heterologous cell systems to express ectopically PAX3/FKHR. Furthermore, most of these studies used clones stably expressing the fusion protein, which precludes discrimination of direct from indirect regulatory events. Nevertheless, a number of potential target genes have been suggested by studies performed in heterologous systems such as c-met (Epstein *et al.*, 1996; Ginsberg *et al.*, 1998), MYCN (Khan *et al.*, 1998), bcl-x1 (Margue *et al.*, 2000), CNR1 and BMP4 (Begum *et al.*, 2005) or CXCR4 (Tomescu *et al.*, 2004). However, the pathophysiological role of these target genes regarding aRMS development or maintenance remains largely unclear.

Therefore, we developed a system to analyse PAX3/FKHR dependent gene expression in aRMS itself. This system consists of two different parts: first, endogenous PAX3/FKHR was downregulated by RNA interference (RNAi) (Elbashir *et al.*, 2001) in aRMS cells in culture

Correspondence: Professor BW Schäfer, Department of Oncology, University Children's Hospital, Steinwiesstrasse 75, Zürich ZH CH-8032, Switzerland.

E-mail: beat.schaefer@kispi.unizh.ch

Received 10 January 2007; revised 2 April 2007; accepted 10 April 2007

followed by gene expression profiling. Second, expression signatures specific for PAX3(7)/FKHR translocations were identified in aRMS tumor biopsies (Wachtel *et al.*, 2004). Comparative expression analysis then was able to identify genes that are dysregulated by PAX3/FKHR both *in vitro* and *in vivo*. Functional studies furthermore revealed that one of these direct target genes, TFAP2B, acts as an essential mediator of PAX3/FKHR function in cell survival.

Results

PAX3/FKHR promotes aRMS cell survival

To characterize PAX3/FKHR target genes relevant for aRMS development and maintenance, we established a small interfering RNA (siRNA)-mediated downregulation strategy. Initially, nine different siRNA molecules against both the PAX3 part and the PAX3/FKHR breakpoint region were tested. siRNAs against the breakpoint region failed to efficiently downregulate the message (data not shown). The remaining siRNA duplexes resulted in specific downregulation efficiencies up to 50% of the original mRNA levels as measured by quantitative reverse transcription (qRT)-PCR. Higher silencing efficiencies were subsequently achieved by different combinations, whereby two siRNAs led to the most effective specific inhibition of 70% in RD eRMS cells and of 80% in Rh4 aRMS cells (Figure 1a). At the protein level, a reduction to 50% of PAX3/FKHR in Rh4 cells and to 40% of PAX3 in RD cells was observed compared to control siRNAs (Figure 1b). No unspecific interferon response was observed (data not shown). Therefore, this combination of siRNAs was used in all silencing experiments. As in translocation-positive aRMS cells alleles for both PAX3 and PAX3/FKHR are present, siRNAs targeting the PAX3 part of the fusion protein could downregulate both PAX3 and PAX3/FKHR. However, we found PAX3 > 1000-fold less expressed than PAX3/FKHR in Rh4 cells suggesting that wild-type PAX3 expression can be neglected (data not shown).

To characterize the physiological effects upon siRNA treatments, proliferation of RD and Rh4 cells after 24, 48 and 72 h of PAX3 silencing was measured. Cell growth was found to be inhibited significantly in cells treated with PAX3 and PAX3/FKHR siRNA, but not in untreated or control treated cells (Figure 1c and d). Furthermore, active caspase-3/7 showed an approximately twofold increase specifically in cells with silenced PAX3 and PAX3/FKHR expression (Figure 1e and f). Thus, an anti-apoptotic function of PAX3 in eRMS and PAX3/FKHR in aRMS cell lines could clearly be demonstrated, as anticipated from earlier findings (Bernasconi *et al.*, 1996). This validates our siRNA approach at the physiological level.

Comparative microarray analysis reveals novel candidate PAX3/FKHR target genes

Next, we sought to identify candidate target genes of PAX3/FKHR using gene expression profiling after

treatment of aRMS cells with siRNA and corresponding controls for 24, 48 and 72 h. As a model system, Rh4 cells were chosen based on previous expression profiling data indicating that Rh4 cells represent most closely *in vivo* biopsies (see Supplementary Materials, Figure 1). The microarray data were analysed using the GeneSpring 7.0 software (Figure 2a). Genes downregulated after 24 h of PAX3/FKHR silencing, and therefore representing putative direct PAX3/FKHR targets, were selected. At the shortest time point of treatment (24 h) at which cellular apoptosis does not yet play a major role 1834 genes were specifically downregulated (> 1.5-fold) when compared to scrambled siRNA (scRNA) treatment (see Supplementary Materials S1). This list of genes identified *in vitro* was then compared to PAX3(7)/FKHR-translocation specific gene signature of 299 genes identified in aRMS tumor biopsies, representing putative *in vivo* PAX3/FKHR target genes (Wachtel *et al.*, 2004). This comparison finally generated an overlapping list of 51 genes, which is statistically highly significant ($P < 0.001$) and not generated simply by chance (Figure 2b and c). These 51 genes therefore represent a transcriptional profile of *in vivo* PAX3/FKHR target genes. They were grouped into different functional classes as indicated in Figure 2d and Table 1. The largest set of genes including FGFR2 and CB1 (CNR1) appear to be involved in signal transduction (25%). Confirming our strategy, CB1 has been recently identified as a direct target of PAX3/FKHR (Begum *et al.*, 2005). The second largest number of genes encode proteins with enzymatic activity (20%). Among them are ADAM10 and ADAM19 metalloproteinases, which might be involved in the enhanced metastatic capability of aRMS cells. Finally, several genes are involved in transcriptional regulation and DNA binding such as the POU domain transcription factor POU4F1 and TFAP2B.

Apart from downregulated genes, we also found a group of genes upregulated 72 h after PAX3/FKHR silencing, suggesting that expression of these genes is normally repressed by PAX3/FKHR. This group comprised 260 genes (see Supplementary Materials S2). Upregulation was specifically observed only starting at 48 h, suggesting an indirect effect of PAX3/FKHR (Figure 3a). Interestingly, genes with most prominent upregulation (up to 58-fold) are all related to normal myogenic differentiation. These included myosin light chain, troponin C, troponin I, crystalline α B and skeletal muscle myosin heavy chain. To confirm these findings, the expression values of two upregulated genes, TNNC2 (34.4-fold) and MYL1 (6.1-fold), were validated by qRT-PCR (Figure 3c). Interestingly, upregulation was specific for aRMS cells and was not detected after downregulation of PAX3 in eRMS cells (Figure 3b and d). Therefore, these experiments support the hypothesis that one of the oncogenic functions of PAX3/FKHR is to block terminal differentiation. Furthermore, they suggest that the cellular background has a profound effect on target genes bound and activated by PAX3 and/or that the target gene spectra of PAX3 and PAX3/FKHR differs (Zhang and Wang, 2006).

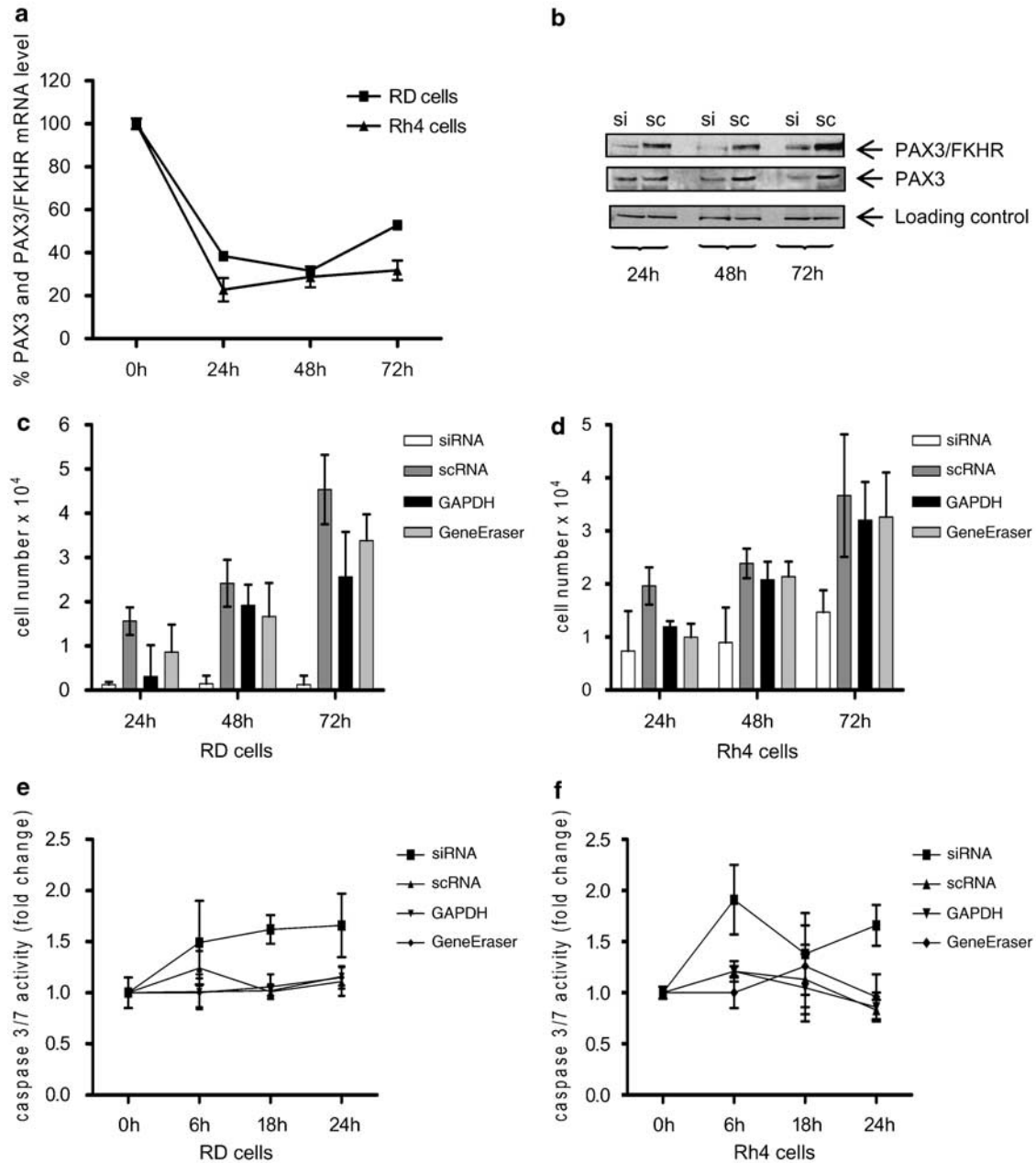


Figure 1 Physiological effects of PAX3 and PAX3/FKHR silencing in RMS cells. (a) mRNA levels of PAX3 and PAX3/FKHR as measured by qRT-PCR analysis after RNAi-mediated downregulation in eRMS (RD) and aRMS (Rh4) cells. The ratio of siRNA to scRNA (control) treatment is shown in %. (b) Protein levels as detected by western blot in 10 μ g of nuclear extract per lane. PAX3/FKHR levels were detected in Rh4 cells, PAX3 levels were detected in RD cells. Cells were treated as indicated with PAX3-specific siRNA (si) or control scRNA (sc). (c and d) Proliferation of RD and Rh4 cells as measured by MTT assay after 72 h of treatment with either PAX3-specific siRNA, scRNA, siRNA targeting GAPDH or transfection reagent alone (GeneEraser). The means \pm s.d. (error bars) from three independent triplicata experiments are shown. (e and f) Induction of apoptosis in RD and Rh4 cells after the indicated time periods of treatment with either PAX3-specific siRNA, scRNA, siRNA targeting GAPDH or GeneEraser (transfection reagent) as measured by caspase-3/7 assay. Fold change values of caspase activity of treated versus non-treated cells from two independent triplicata experiments. eRMS, embryonal RMS; GAPDH, glyceraldehyde-3-phosphate dehydrogenase; MTT, 3-(4,5-dimethylthiazol-2-yl)-2,5-diphenyltetrazolium bromide; qRT-PCR, quantitative reverse transcription-PCR; RMS, rhabdomyosarcoma; siRNA, small interfering RNA.

TFAP2B is a direct target gene of *PAX3/FKHR*
One of the oncogenic functions of *PAX3/FKHR* is promotion of cell survival. Therefore, it was surprising that no classic apoptotic genes could be identified in our system. However, one of the potential target genes,

TFAP2B, has previously been implicated in apoptosis in a mouse model (Moser *et al.*, 1997). We, therefore, further characterized this potential target gene, first by verification of the microarray expression levels after siRNA treatment by qRT-PCR with *CB1* as a control (Figure 4a).

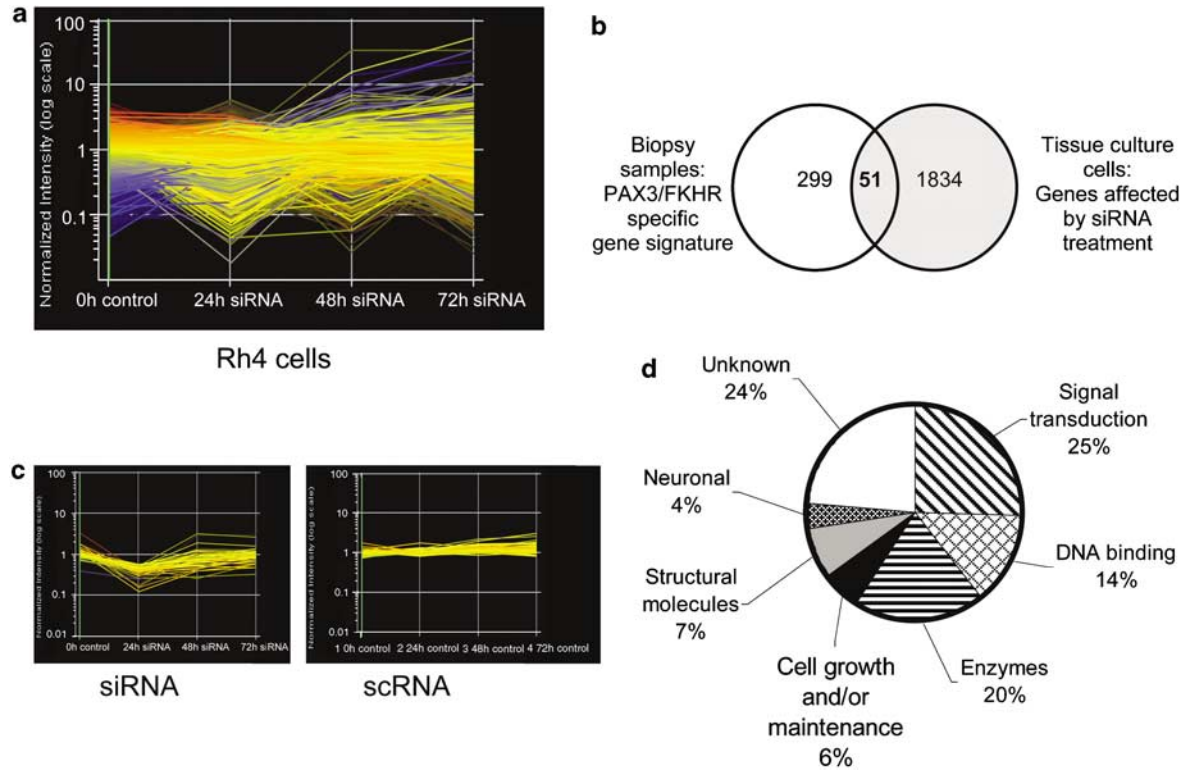


Figure 2 Changes in gene expression after PAX3/FKHR silencing and identification of PAX3/FKHR target genes in aRMS cells. **(a)** Diagram depicting normalized expression values (log₁₀ scale) of 16221 filtered genes as measured in Rh4 cells after 0, 24, 48 and 72 h of treatment with PAX3-specific siRNA. Each line represents the expression of one gene. **(b)** Diagram depicting the overlap between a PAX3(7)/FKHR-specific gene signature derived from aRMS biopsies and genes downregulated by PAX3-specific siRNA treatment in Rh4 cells: 51 genes are present in both signatures. **(c)** Temporal changes of expression levels of the 51 genes identified in **(b)** in Rh4 cells after 0, 24, 48 and 72 h of treatment with PAX3-specific siRNA or scRNA. **(d)** Graphic representation depicting the ontology of the 51 potential PAX3/FKHR target genes identified in **(b)**. A complete list of the functions as well as downregulation levels of the 51 genes is shown in Table 1. aRMS, alveolar RMS; RMS, rhabdomyosarcoma; scRNA, scrambled siRNA; siRNA, small interfering RNA.

Next, we studied the impact of PAX3/FKHR on transcription of these genes in 293T cells, which normally express neither CB1 nor TFAP2B at substantial levels. As expected, after ectopical expression of PAX3/FKHR, transcription of both endogenous genes was induced ~5-fold (Figure 4b). To test whether direct DNA binding is necessary, we used PAX3/FKHR mutants in which either the paired or the homeodomain DNA-binding domain contains inactivating point mutations (Xia and Barr, 2004). Interestingly, CB1 transcription was not induced by the mutant bearing a non-functional homeodomain, whereas TFAP2B transcription was not induced by the mutant with an impaired-paired domain. We therefore conclude that activation of CB1 depends mainly on the PAX3 homeodomain, and that of TFAP2B however on the paired domain (Figure 4b). Full transcriptional activation, however, can only be reached using the intact PAX3/FKHR protein.

To identify potential paired domain binding sites in the TFAP2B promoter, 3200 bp upstream of the transcriptional start site and deletion constructs thereof were cloned in front of a luciferase reporter and used in reporter assays in 293T cells. PAX3/FKHR induced a significant transactivation of up to threefold compared to control with the full-length as well as a shorter 1.5 kb

(deletion construct 1, TFAP2b_1) reporter construct (Figure 4c). Further deletion down to 0.8 kb (deletion construct 2, TFAP2b_2) reduced transactivation significantly. Transactivation of the 1.5 kb construct was also dependent on an intact paired domain as observed before (Figure 4d). Therefore, these experiments suggested a potential binding site for the PAX3/FKHR paired domain between -1592 and -806 bp. To verify these results, we next performed a chromatin immunoprecipitation (ChIP) experiment to test for direct binding of PAX3/FKHR to this promoter region. Deletion constructs 1 and 2 were cotransfected with a His-tagged PAX3 construct into 293T cells and immunoprecipitated with either control IgG or specific anti-His antibodies. We recovered a twofold higher amount of TFAP2B promoter DNA from the specific immunoprecipitation of deletion construct 1 compared to the control but not of deletion construct 2. These experiments verify that PAX3/FKHR can bind to the TFAP2B promoter in the region -1592 to -806 (Figure 4e). In this region, three potential PAX3/FKHR-binding sites at positions -1461, -1252 and -1186 were identified (Figure 4f). Using site-directed mutagenesis these sites were deleted individually and tested in a reporter assay. Whereas promoter fragments

Table 1 Ontology and downregulation levels of 51 potential PAX3/FKHR target genes

<i>Gene name</i>	<i>Common</i>	<i>Description</i>	<i>Downregulation 24 h (fold)</i>	<i>Function</i>
<i>Signal transduction</i>				
207232_s_at	DZIP3	Zinc-finger DAZ interacting protein 3	6.1	Ligase activity, protein ubiquitination, RNA binding, zinc ion binding
220197_at	ATP6V0A4	ATPase, H ⁺ transporting, lysosomal V0 subunit a isoform 4	5.7	Ion transport, proton transport, regulation of pH
204882_at	ARHGAP25	Rho GTPase-activating protein 25	4.2	GTPase activator activity
203638_s_at	FGFR2	Fibroblast growth factor receptor 2 (bacteria-expressed kinase, keratinocyte growth factor receptor, craniofacial dysostosis 1, Crouzon syndrome, Pfeiffer syndrome, Jackson-Weiss syndrome)	3.2	Cell growth, protein amino-acid phosphorylation
206723_s_at	EDG4	Endothelial differentiation, lysophosphatidic acid G-protein-coupled receptor, 4	2.9	G-protein coupled receptor protein signaling pathway, lysophingolipid and lysophosphatidic acid receptor activity, lipid binding
212915_at	SEMACAP3	Likely ortholog of mouse semaF cytoplasmic domain associated protein 3	2.7	Metal ion binding, protein ubiquitination, ubiquitin-protein ligase activity
203233_at	IL4R	Interleukin 4 receptor	2.6	Immune response, receptor signaling protein activity
209869_at	ADRA2A	Adrenergic, α -2A-, receptor	2.5	Activation of MAPK activity, Ras protein signal transduction, positive regulation of cell proliferation
213436_at	CNR1; CB1; CB-R; CB1A; CANN6; CB1K5	Cannabinoid receptor 1 (brain)	2.3	Cannabinoid receptor activity, G-protein signaling, coupled to cyclic nucleotide second messenger
205068_s_at	GRAF	GTPase regulator associated with focal adhesion kinase pp125 (FAK)	1.9	Nervous system development, Rho GTPase activator activity
221578_at	RASSF4	RAS association (RalGDS/AF-6) domain family 4	1.8	Oxidoreductase activity
200972_at	TM4SF8	Transmembrane 4 superfamily member 8	1.7	Cell motility, cell proliferation
218373_at	FTS	Fused toes homolog (mouse)	1.6	Apoptosis, ubiquitin-like activating enzyme activity
<i>DNA binding</i>				
202320_at	GTF3C1	General transcription factor IIIC, polypeptide 1, α 220 kDa	9.6	DNA binding, RNA polymerase III transcription factor activity, rRNA transcription, tRNA transcription
205935_at	FOXF1	Forkhead box F1	2.8	Regulation of transcription, DNA-dependent; regulation of transcription from Pol II promoter
209757_s_at	MYCN	V-myc myelocytomatosis viral related oncogene, neuroblastoma derived (avian)	2.8	Transcription factor activity, protein binding, regulation of transcription, DNA-dependent
206940_s_at	POU4F1	POU domain, class 4, transcription factor 1	2.7	Development, transcription factor activity, regulation of transcription from Pol II promoter
218445_at	H2AFY2	H2A histone family, member Y2	2.6	Dosage compensation
214451_at	TFAP2B	Transcription factor AP-2 β (activating enhancer binding protein 2 β)	2.6	Nervous system development, transcription factor activity, transcription coactivator activity
211341_at	POU4F1	POU domain, class 4, transcription factor 1	2.4	Development, transcription factor activity, regulation of transcription from Pol II promoter
<i>Enzymes</i>				
212989_at	MOB	Mob protein	3.4	Kinase activity, lipid metabolism, transferase activity
214961_at	KIAA0774	KIAA0774	3.1	Catalytic activity
221605_s_at	PIPOX	Pipecolic acid oxidase	3.0	Electron transport, oxidoreductase activity, tetrahydrofolate metabolism
206447_at	ELA1	Elastase 1, pancreatic	3.0	Trypsin activity, pancreatic elastase activity, hydrolase activity
209460_at	ABAT	4-Aminobutyrate aminotransferase	2.9	Transferase activity, neurotransmitter catabolism
209765_at	ADAM19	A disintegrin and metalloproteinase domain 19 (meltrin β)	2.5	Hydrolase activity; metalloendopeptidase activity, proteolysis
212006_at	UBXD2	UBX domain containing 2	2.3	Regulation of transcription, DNA-dependent, transcription factor activity

Table 1 (continued)

Gene name	Common	Description	Downregulation 24 h (fold)	Function
204074_s_at	KIAA0562	Glycine-, glutamate-, thienylcyclohexylpiperidine-binding protein	2.2	Binding, hydrolase activity
205811_at	POLG2	Polymerase (DNA directed), γ 2, accessory subunit	1.9	DNA repair, DNA-dependent DNA replication, protein biosynthesis, metallopeptidase activity
202603_at	ADAM10	A disintegrin and metalloproteinase domain 10	1.9	Hydrolase activity, protein amino-acid phosphorylation, metalloendopeptidase activity
<i>Cell growth and/or maintenance</i>				
205430_at	BMP5	Continued from bA120K22.1 in Em:AL137178 match: proteins: Tr:Q9YGH7 Sw:P22003 Sw:P22004 Sw:P20722 Tr:Q91403 Sw:P30886 Sw:P49003 Sw:Q04906 Sw:P18075 Sw:P23359; human DNA sequence from clone RP1-181C24 on chromosome 6p11.1-12.2 contains the 3' end of the BM	6.2	Cell differentiation, cytokine activity, growth, growth factor activity, skeletal development
209814_at	ZNF330	Zinc-finger protein 330	2.9	Metal ion binding, protein binding, zinc ion binding
203651_at	ZFYVE16	Zinc finger, FYVE domain containing 16	1.9	Endosome transport, metal ion binding, protein targeting to lysosome, regulation of endocytosis, vesicle organization and biogenesis
<i>Structural molecules</i>				
221854_at	PKP1	Plakophilin 1 (ectodermal dysplasia/skin fragility syndrome)	8.0	Cell-cell signaling, cell adhesion
203256_at	CDH3	Cadherin 3, type 1, P-cadherin (placental)	6.0	Cell adhesion, calcium ion binding
203072_at	MYO1E	Myosin IE	2.1	Actin binding, ATP binding, ATPase activity, actin filament-based movement
211059_s_at	GOLGA2	Golgi autoantigen, golgin subfamily a, 2	1.7	Protein binding
<i>Neuronal</i>				
206089_at	NELL1	NEL-like 1 (chicken)	4.7	Nervous system development, cell adhesion
204105_s_at	NRCAM	Neuronal cell adhesion molecule	3.5	Ankyrin binding, cell-cell adhesion, neuron migration, positive regulation of neuron differentiation, protein binding, synaptogenesis
<i>Unknown</i>				
210102_at	LOH11CR2A	Loss of heterozygosity, 11, chromosomal region 2, gene A	2.7	Unknown
221185_s_at	DKFZp434-B227	Synonyms: FLJ11667, FLJ23571; Homo sapiens hypothetical protein DKFZp434B227 (DKFZp434B227), mRNA.	2.6	Unknown
205888_s_at	KIAA0555	KIAA0555 gene product	2.5	Unknown
213179_at		602381329F1 NIH_MGC_93 Homosapiens cDNA clone IMAGE:4499023 5', mRNA sequence.	2.4	Unknown
209693_at	ASTN2	Astrotactin 2	2.4	Unknown
219438_at	FLJ12650	Hypothetical protein FLJ12650	2.3	Unknown
220610_s_at	LRRFIP2	Leucine rich repeat (in FLII) interacting protein 2	2.3	Unknown
207759_s_at	FLJ41105	Hypothetical gene supported by AK123100	2.2	Unknown
49111_at		MRNA; cDNA DKFZp762M127 (from clone DKFZp762M127)	2.2	Unknown
43511_s_at		MRNA; cDNA DKFZp762M127 (from clone DKFZp762M127)	1.9	Unknown
212736_at	BC008967	Hypothetical gene BC008967	1.8	Unknown
219225_at	PGBD5	PiggyBac transposable element derived 5	1.6	Unknown

with deletion of the site -1461 (deletion 1) could be activated > 3-fold, deletion of the six nucleotides GTTCCG at position -1252 bp (deletion 2) reduced the transactivation potential of PAX3/FKHR to background levels. As this motif has previously been

described as binding motif for paired domains (Mayanil *et al.*, 2001), it represents a likely binding site for the PAX3/FKHR paired domain. Deletion 3 at position -1186 also showed reduced activity (twofold), suggesting that this site plays an assistant role.

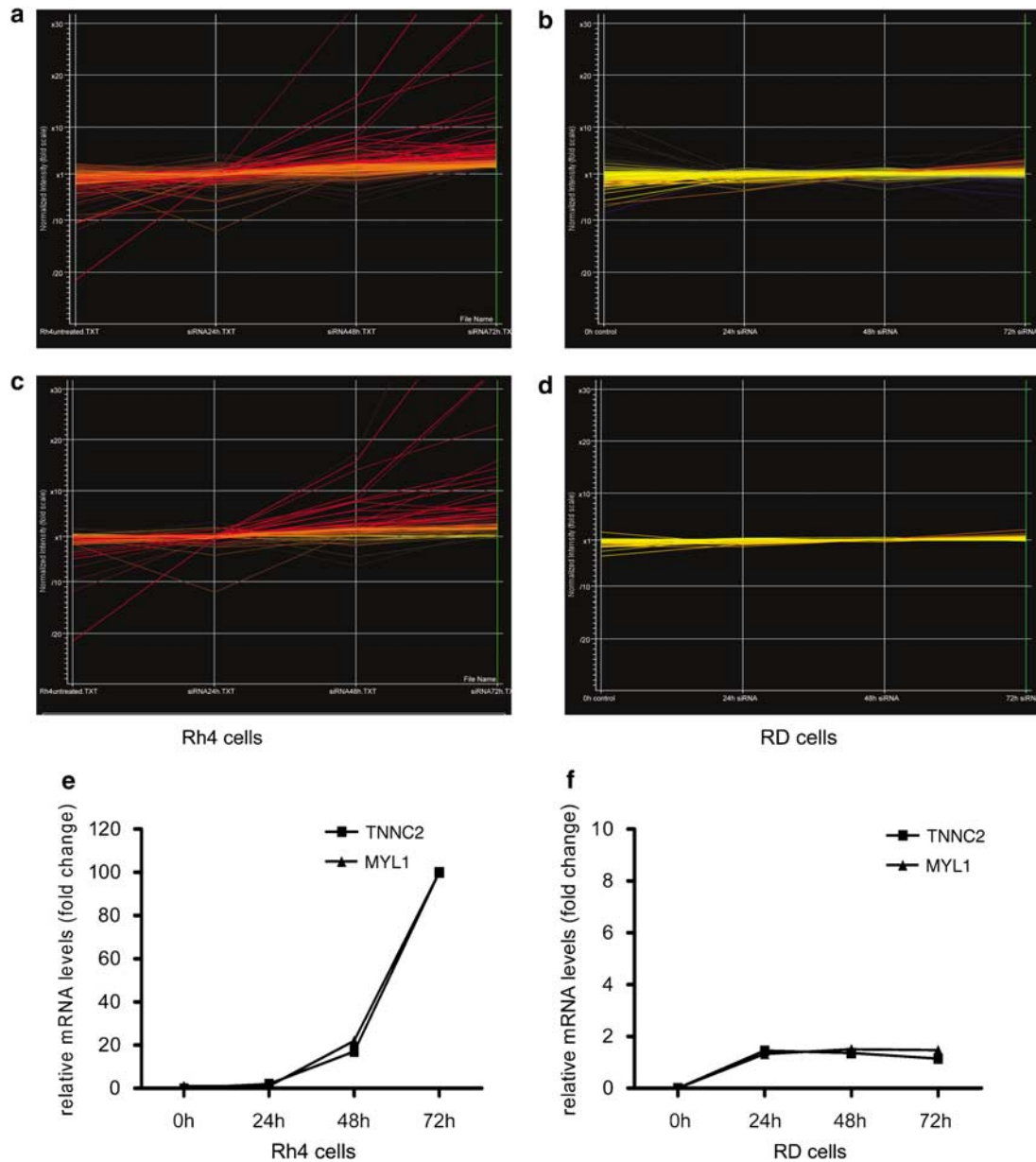


Figure 3 Upregulated genes after silencing of PAX3 and PAX3/FKHR in RMS cells. **(a)** Diagram depicting expression values (fold change scale) of 260 genes upregulated more than twofold in Rh4 cells after 72 h of PAX3-specific siRNA treatment. **(b)** Expression levels of the same set of genes as in **(a)** in RD cells. Expression values were calculated in relation to scRNA treatment; levels of upregulation are listed in Supplementary Table 2. **(c)** Diagram depicting the expression values (fold change scale) of 52 genes (represented by 67 probe sets) involved in muscle development, which are upregulated in Rh4 cells after silencing of PAX3/FKHR for 72 h. Levels of upregulation are listed in Table 2. **(d)** Diagram depicting the expression values of the same 52 genes as in **(c)** in RD cells after 72 h of PAX3 silencing. **(e and f)** Verification of the expression changes of two genes, TNNC2 and MYL1, by qRT-PCR analysis. Fold change values in siRNA compared to scRNA-treated cells are shown. qRT-PCR, quantitative reverse transcription-PCR; RMS, rhabdomyosarcoma; scRNA, scrambled siRNA; siRNA, small interfering RNA.

To confirm these data, an electrophoretic mobility shift assay was performed with double-stranded oligonucleotides corresponding to deletion sites 2 (Figure 4h) and 3 (data not shown). As expected, DNA-protein binding could be observed after ectopical expression of His-tagged PAX3 and was comparable when using PAX3/FKHR (data not shown). Furthermore, DNA-protein binding with the oligonucleotide specific for

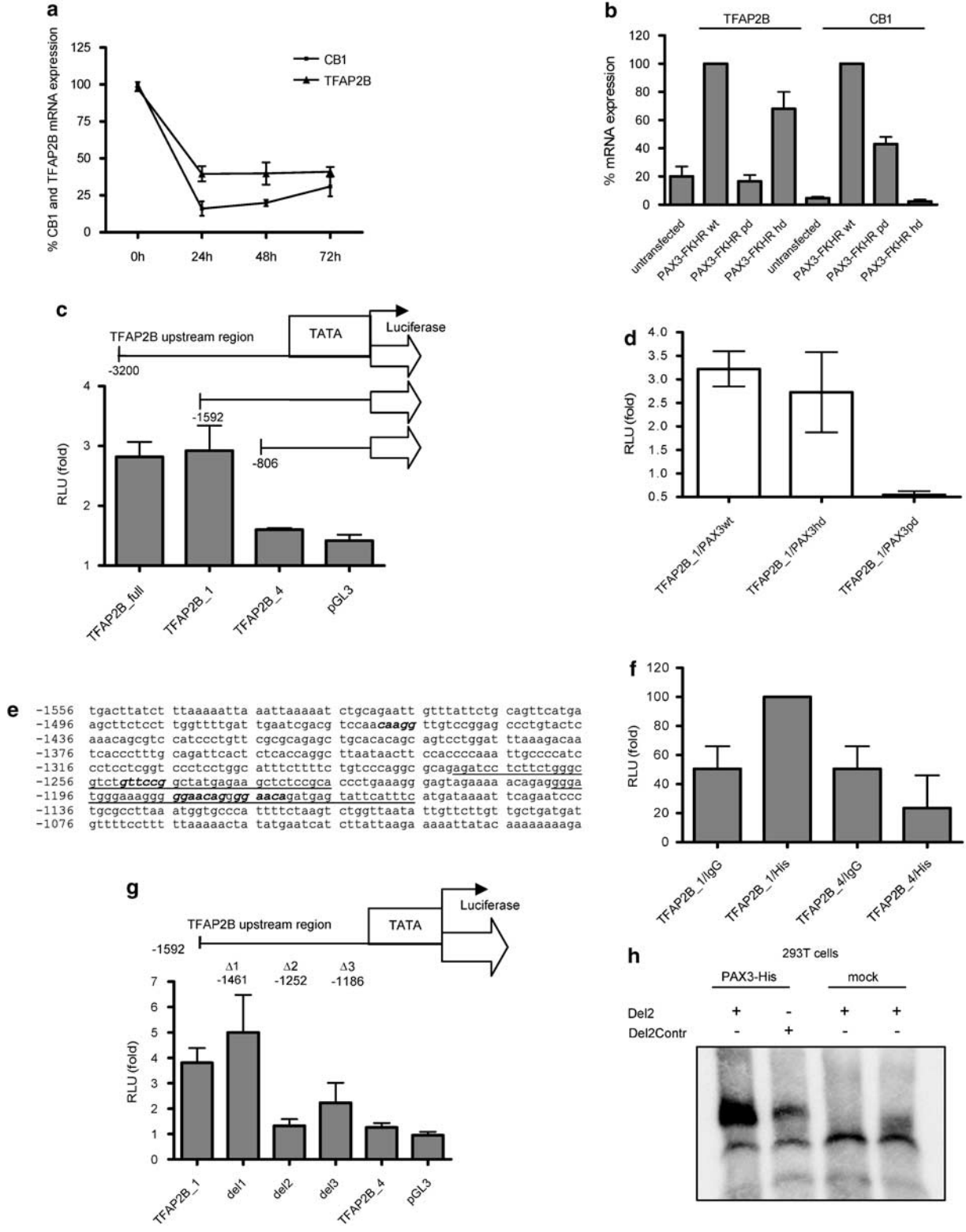
deletion site 3 was considerably weaker, consistent with the observation made with reporter deletion constructs (Figure 4g).

We conclude from these experiments that TFAP2B is a novel direct target gene of PAX3/FKHR whose transactivation is dependent on two DNA-binding motifs recognized by the PAX3 paired domain at positions -1252 and -1186 bp.

TFAP2B mediates anti-apoptotic function of *PAX3/FKHR*

TFAP2B has been shown to suppress *myc*-induced programmed cell death in a range of cell lines (Moser *et al.*, 1997). Therefore, we hypothesized that the

pro-survival function of *PAX3/FKHR* might depend on expression of *TFAP2B* as a *PAX3/FKHR* target gene. To test this hypothesis, we first investigated the effects of specific *TFAP2B* silencing on cell survival. siRNA-mediated silencing of *TFAP2B* resulted in



efficient downregulation of TFAP2B expression on mRNA (80%) as well as on protein (50–60%) level (Figure 5a and b). Downregulation of TFAP2B resulted in suppression of cell proliferation, not observed in control treated cells. Importantly, specific siRNA treatment also increased the rate of apoptosis as measured by an increase in caspase-3/7 activity by 1.7-fold (Figure 5d). The number of apoptotic cells significantly increased from 3 to 41% (Figure 5e), an increase very similar to the result observed after PAX3/FKHR silencing (3–36%). These experiments suggest that the anti-apoptotic function of PAX3/FKHR might be mediated, at least in part, by direct transcriptional activation of TFAP2B.

To test this directly, Rh4 cells stably overexpressing TFAP2B from a heterologous promoter were generated. PAX3/FKHR was downregulated by siRNA treatment and cell proliferation and apoptosis rate measured as before. In these cells proliferation was rescued to almost normal levels (Figure 6a) and the number of dead cells increased only slightly (1.6-fold) whereas dead cells increased 5.1-fold in non-transfected and 3.5-fold in mock-transfected Rh4 cells (Figure 6b). We conclude from these experiments that TFAP2B acts downstream of PAX3/FKHR to mediate, at least part, of its anti-apoptotic function and therefore represents an essential target gene of PAX3/FKHR.

Discussion

The identification of physiologically relevant PAX3/FKHR target genes is crucial for understanding the oncogenic function of this chimeric transcription factor. Analysis of target genes has been hampered by the use of heterologous cell systems to study the fusion protein. Here, we used patient-derived aRMS cells to analyse PAX3/FKHR target genes using a loss-of-function silencing approach, in parallel to data acquired from tumor biopsies. This approach allowed the identification of a large set of bona fide PAX3/FKHR target genes.

The choice of aRMS cells to be used as a model system was important and based on previous expression profiling data. These indicated that Rh4 cells most closely reflect *in vivo* biopsies and therefore are best suited to serve as model for aRMS tumors (Wachtel *et al.*, 2004). Similar to other aRMS cells (Bernasconi *et al.*, 1996; Ayyanathan *et al.*, 2000), we found that ongoing expression of PAX3/FKHR is required for Rh4 cell survival, suggesting that aRMS cells are 'addicted' to PAX3/FKHR expression. Measuring changes in the transcriptome at different time points after silencing of PAX3/FKHR revealed a set of genes whose expression is downregulated in parallel with PAX3/FKHR, and was therefore analysed in more detail.

Interestingly, at 24 h after silencing only downregulated genes were identified, which is in agreement with the observation that PAX3/FKHR mainly acts as transcriptional activator. Within the subset of potential PAX3/FKHR target genes, already known targets were present, like CB1 (Begum *et al.*, 2005), MYCN (Khan *et al.*, 1998) and NCAM (Edelman and Jones, 1995), thus confirming our strategy. To constrict the list to those genes relevant *in vivo*, the set was compared to a PAX3(7)/FKHR-translocation specific gene signature identified directly from aRMS tumor biopsies. From this comparison, we identified a subset of 51 overlapping genes, which are likely to represent relevant PAX3/FKHR targets important for the oncogenic properties of the fusion protein. The comparative expression profiling therefore revealed a large amount of novel biological information. In a very recent study, Davicioni *et al.* (2006) measured the expression profiles after expression of PAX3/FKHR in the related eRMS cell line RD and compared this gene set to data from tumor biopsies. Of the 61 potential target genes identified in their study, 9 are identical with genes identified in our study, namely ABAT, ADAM10, BMP5, IL4R, KIAA0555, MYCN, NELL1, NRCAM and POU4F1. In addition, another three genes (TFAP2B, CDH3 and CNR1) were excluded in their analysis only because transcriptional activation

Figure 4 Targeting of the TFAP2B promoter by PAX3/FKHR. (a) mRNA levels of TFAP2B and CB1 were measured by qRT-PCR in Rh4 cells at indicated time points after RNAi-mediated PAX3/FKHR downregulation. The ratio of siRNA to scRNA treatment is shown in %. (b) mRNA levels of TFAP2B and CB1 in 293T cells, either untransfected or transfected with the indicated PAX3/FKHR construct, as measured by qRT-PCR. PAX3hd and PAX3pd are homeodomain- and paired domain-specific mutants of PAX3/FKHR. (c) Deletion analysis of the TFAP2B promoter. A luciferase reporter construct containing the 3200 bp upstream of the TFAP2B transcriptional start site (TFAP2B_full) or deletion constructs thereof, containing remaining parts of 1592 bp (TFAP2B_1) or 806 bp (TFAP2B_2), respectively, are shown schematically in the upper panel. Transactivation of PAX3/FKHR on the different constructs as measured by luciferase assays is shown in the lower panel. The means \pm s.d. (error bars) from two independent duplicate experiments are shown (RLU, relative light units). (d) Transactivation of the indicated PAX3/FKHR constructs on deletion construct TFAP2B_1 as measured by luciferase assay. (e) Sequences of three potential PAX3/FKHR binding sites within the TFAP2B promoter region. Commonly described motifs for paired domain binding are indicated by bold cursive type. Sequences for the design of oligonucleotides used for EMSA are underlined. (f) Binding of PAX3 to the promoter regions of the TFAP2B_1 and TFAP2B_2 deletion constructs as detected by chromatin immunoprecipitation (ChIP). His-tagged PAX3 protein/DNA complexes were immunoprecipitated with α -His antibody or unspecific mouse IgG. qRT-PCR quantification of precipitated DNA of each experiment ($n=3$) was performed in triplicates and values from the anti-His immunoprecipitation were normalized with the values from the control immunoprecipitation with IgG. (g) Schematic representation of single deletions of possible binding sites of PAX3/FKHR in TFAP2B_1 as introduced by site-directed mutagenesis is shown in the upper panel. Luciferase activity of the indicated deletion constructs as measured after cotransfection with PAX3/FKHR in 293T cells. Each bar represents means \pm s.d. from three independent duplicate experiments. (h) EMSA used for measurement of DNA-binding properties of PAX3 against the deletion site 2 in the promoter region of TFAP2B. The assay was performed with 8 μ l of nuclear protein extracted after transfection of PAX3-His in 293T cells. As control, mock-transfected 293T cells and mismatch oligonucleotides were used. EMSA, electrophoretic mobility shift assay; qRT-PCR, quantitative reverse transcription-PCR; scRNA, scrambled siRNA; siRNA, small interfering RNA.

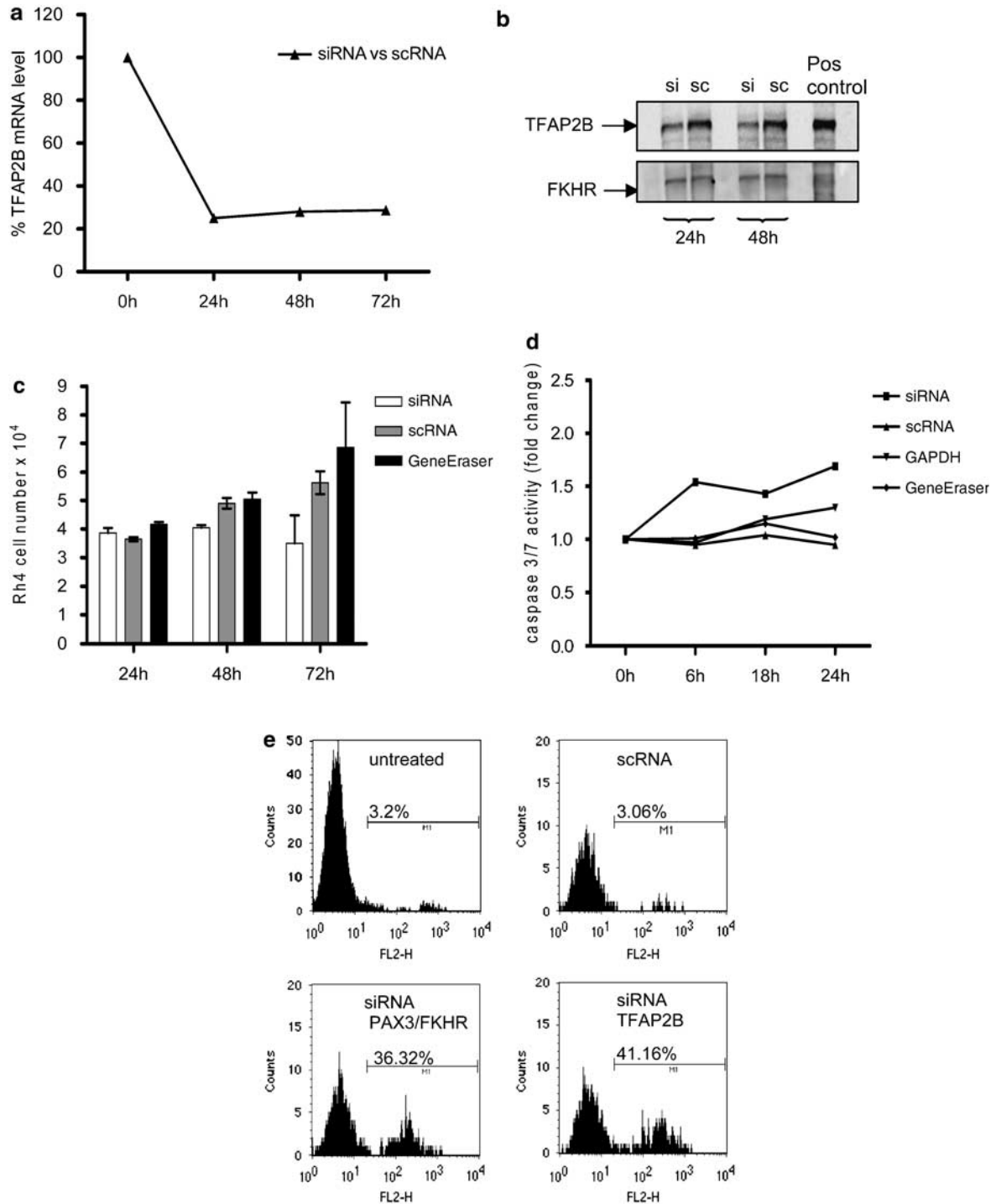
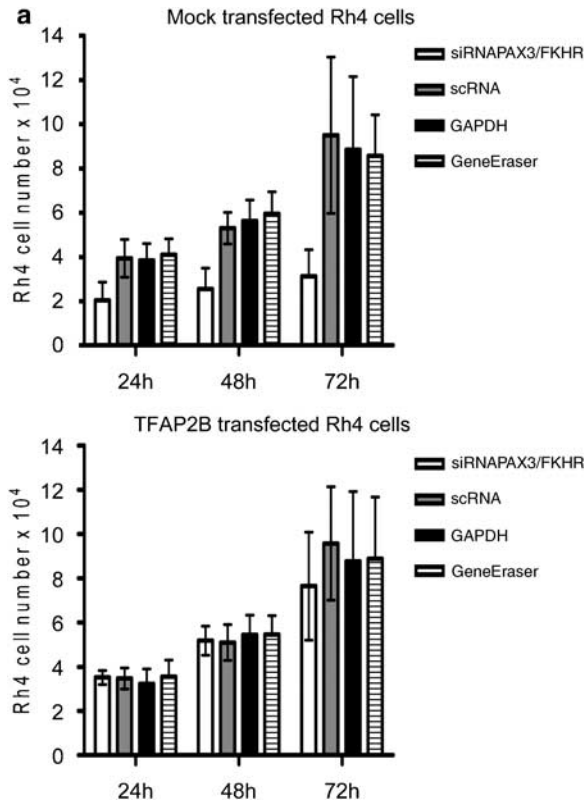


Figure 5 Physiological effects of TFAP2B silencing in aRMS cells. **(a)** mRNA level of TFAP2B after RNAi-mediated downregulation in Rh4 cells as measured by qRT-PCR analysis. The ratio of siRNA to scRNA (control) treatment is shown. **(b)** Protein levels of TFAP2B as determined by western blot with 10 μ g of nuclear protein from TFAP2B specific – (si) and control siRNA (sc) treated cells extracted 24 and 48 h after transfection. In the positive control lane, mTFAP2B transiently overexpressed in 293T cells is shown as size control. FKHR protein levels were used as loading control. **(c)** Cell proliferation as measured by MTT assay after different time periods of treatment with TFAP2B-specific siRNA, scRNA and transfection reagent alone (GeneEraser). The means \pm s.d. (error bars) from three independent triplicate experiments are shown. **(d)** Apoptosis rate in Rh4 cells transfected with the indicated siRNA as detected by a caspase-3/7 assay at the indicated time points. Mean values of one representative experiment performed in triplicates are shown. **(e)** Histogram plots of FACS results of cells stained with PI 24 h after treatment with the indicated siRNA. Percentages of PI-positive cells are depicted above the horizontal bars. aRMS, alveolar RMS; qRT-PCR, quantitative reverse transcription-PCR; MTT, 3-(4,5-dimethylthiazol-2-yl)-2,5-diphenyltetrazolium bromide; PI, propidium iodide; RMS, rhabdomyosarcoma; scRNA, scrambled siRNA; siRNA, small interfering RNA.



b

Cell line	Treatment	Apoptosis rate (% PI positive cells)	Apoptosis rate (fold change siRNA vs control)
Rh4	PAX3/FKHR silencing	46%	5.1
Rh4	control	9%	
Rh4 mock	PAX3/FKHR silencing	35%	3.5
Rh4 mock	control	10%	
Rh4 mTFAP2B	PAX3/FKHR silencing	21%	1.6
Rh4 mTFAP2B	control	13%	

Figure 6 Physiological link between PAX3/FKHR and TFAP2B. (a) Cell proliferation of mock-transfected Rh4 cells and cells stably overexpressing mTFAP2B as measured by MTT assay at indicated time points after PAX3/FKHR silencing. Treatment with siRNA specific for PAX3/FKHR was compared to scRNA, siRNA targeting GAPDH and GeneEraser alone. (b) Comparison of apoptosis rates in parental Rh4 cells, Rh4 cells stably overexpressing TFAP2B and mock-transfected Rh4 cells as measured by FACS of PI-stained cells 24 h after downregulation of PAX3/FKHR. GAPDH, glyceraldehyde-3-phosphate dehydrogenase; MTT, 3-(4,5-dimethylthiazol-2-yl)-2,5-diphenyltetrazolium bromide; PI, propidium iodide; scRNA, scrambled siRNA; siRNA, small interfering RNA.

in RD cells was below the defined threshold level. This again underscores the validity of our approach.

Performing ontology studies, six main groups of target genes were identified, such as genes encoding for receptors, among them FGFR2 or IL4R, which are obvious candidates as therapeutic targets. Moreover, genes like NCAM, ADRA2A, POU4F1 or BMP5 could elucidate pathways involved in cell development and differentiation in aRMS. Other characteristics of aRMS tumors may be the result of other targets of PAX3/FKHR, such as ADAM 10 and ADAM 19, which could play a role in enhanced metastatic potential of aRMS cells, a crucial property of the alveolar subtype.

Interestingly, 72 h after siRNA treatment a set of genes upregulated in Rh4, but not in RD cells was identified, suggesting a specific repressing effect of PAX3/FKHR. This set included numerous genes related to muscle differentiation (see Table 2). There are different possible explanations for this observation: first, PAX3/FKHR could upregulate a transcriptional repressor, whereby repression would be an indirect effect, consistent with the time point (72 h) at which expression changes were identified. Alternatively PAX3/FKHR is directly involved in repressing myogenic differentiation, which is consistent with the oncogenic

role of this transcription factor. This differentiation-repressing activity of PAX3/FKHR is supported by recent studies, where PAX3 was shown to play a role in both initiation of the melanogenic cascade while preventing at the same time terminal differentiation in melanocyte stem cells (Lang *et al.*, 2005). The precise mechanism how PAX3/FKHR accomplishes this differentiation barrier in aRMS is not clear. However, in our study expression levels of well-known factors in the myogenic differentiation pathway downstream of PAX3 such as myogenin or MyoD were too low to be detected on our microarrays.

Among the target genes identified, which are interesting candidates to transduce the oncogenic effects of PAX3/FKHR, was TFAP2B. It belongs to a transcription factor family consisting of four members, which are known to be coexpressed in early premigratory and migrating neural crest cells. Moreover, TFAP2B has been shown to play a role in apoptosis and survival of epithelial cells in collecting ducts and distal tubuli in mice embryonic tissue (Moser *et al.*, 1997, 2003). Since PAX3/FKHR is also involved in regulation of cell survival, TFAP2B was confirmed at the molecular level as a direct target of PAX3/FKHR. The use of PAX3/FKHR mutants with impaired DNA-binding activity demonstrated paired domain dependency of TFAP2B

Table 2 Upregulation levels of 52-muscle development related genes represented by 67 probe sets

Gene name	Common	Description	Rh4 fold change upregulation si versus sc	RD fold change upregulation si versus sc
209904_at	TNNC1	Troponin C, slow	58.2	0.8
205163_at	HUMMLC2B	Myosin light chain 2	37.1	0.9
205388_at	TNNC2	Troponin C2, fast	34.4	1.0
206304_at	MYBPH	Myosin binding protein H	22.4	1.0
205940_at	MYH3	Myosin, heavy polypeptide 3, skeletal muscle, embryonic	21.6	0.6
206393_at	TNNI2	Troponin I, skeletal, fast	18.4	0.8
221994_at	PDLIM5	LIM protein (similar to rat protein kinase C-binding enigma)	15.1	0.9
214122_at	PDLIM7	PDZ and LIM domain 7 (enigma)	14.2	1.2
210329_s_at	SGCD	Sarcoglycan, δ (35 kDa dystrophin-associated glycoprotein)	12.6	1.3
209283_at	CRYAB	Crystallin, α B	9.6	1.0
205951_at	MYH1	Myosin, heavy polypeptide 1, skeletal muscle, adult	9.5	5.1
219772_s_at	SMPX	Small muscle protein, X-linked	8.6	1.1
205730_s_at	ABLIM3	Go_function: actin binding (goid 0003779) (evidence IEA); go_process: cytoskeleton organization and biogenesis (goid 0007010) (evidence IEA); Homo sapiens actin binding LIM protein family, member 3 (ABLIM3), mRNA.	8.3	0.9
206394_at	MYBPC2	Myosin binding protein C, fast type	7.7	3.9
34471_at	MYH8	Myosin, heavy polypeptide 8, skeletal muscle, perinatal	7.4	1.5
213023_at	UTRN	Utrophin (homologous to dystrophin)	7.2	1.3
205610_at	MYOM1	Myomesin 1 (skelemin) 185 kDa	6.3	1.0
206116_s_at	TPM1	Tropomyosin 1 (α)	6.2	0.7
209888_s_at	MYL1	Myosin, light polypeptide 1, alkali; skeletal, fast	6.1	1.0
200974_at	ACTA2	Actin, α 2, smooth muscle, aorta	5.9	0.8
218736_s_at	PALMD	Palmdelphin	5.9	1.1
201438_at	COL6A3	Collagen, type VI, α 3	5.8	1.2
206538_at	MRAS	Muscle RAS oncogene homolog	5.6	3.5
210298_x_at	FHL1	Four and a half LIM domains 1	5.3	1.0
210395_x_at	MYL4	Myosin, light polypeptide 4, alkali; atrial, embryonic	5.3	0.6
216054_x_at	MYL4; GT1; ALC1; AMLC; PRO1957	Human MLC1emb gene for embryonic myosin alkaline light chain, promoter and exon 1.	5.2	0.5
205693_at	TNNI3	Troponin T3, skeletal, fast	5.1	0.7
210088_x_at	MYL4	Myosin, light polypeptide 4, alkali; atrial, embryonic	5.1	0.5
210330_at	SGCD	Sarcoglycan, δ (35 kDa dystrophin-associated glycoprotein)	5.0	2.1
206717_at	MYH8	Myosin, heavy polypeptide 8, skeletal muscle, perinatal	5.0	1.4
217585_at	NEBL	Nebulette	4.8	1.0
210202_s_at	BIN1	Bridging integrator 1	4.6	0.8
205547_s_at	TAGLN	Transgelin	4.5	0.8
203037_s_at	MTSS1	Metastasis suppressor 1	4.2	1.0
207317_s_at	CASQ2	Calsequestrin 2 (cardiac muscle)	4.1	1.1
213371_at	LDB3	LIM domain binding 3	4.1	0.7
203821_at	DTR	Diphtheria toxin receptor (heparin-binding epidermal growth factor-like growth factor)	4.0	0.5
214087_s_at	MYBPC1	Myosin binding protein C, slow type	4.0	1.0
203243_s_at	PDLIM5	LIM protein (similar to rat protein kinase C-binding enigma)	4.0	1.0
205177_at	TNNI1	Troponin I, skeletal, slow	3.9	0.7
207302_at	SGCG	Sarcoglycan, γ (35 kDa dystrophin-associated glycoprotein)	3.9	1.1
204173_at	MLC1SA	Myosin light chain 1 slow a	3.8	0.9
206117_at	TPM1	Tropomyosin 1 (α)	3.5	0.7
201976_s_at	MYO10	Myosin X	3.4	1.0
202931_x_at	BIN1	Bridging integrator 1	3.3	0.9
214492_at	SGCD	Sarcoglycan, δ (35 kDa dystrophin-associated glycoprotein)	3.1	1.3
219829_at	ITGB1BP2	Integrin β 1 binding protein (melusin) 2	3.1	0.3
217274_x_at	MYL4; GT1; ALC1; AMLC; PRO1957	Skeletal embryonic form; H sapiens skeletal embryonic myosin light chain 1 (MLC1) mRNA	2.8	0.7
215279_at	SVIL	Supervillin	2.7	1.1
213717_at	LDB3	LIM domain binding 3	2.6	1.0
204533_at	CXCL10	Chemokine (C-X-C motif) ligand 10	2.5	1.2
213022_s_at	UTRN	Utrophin (homologous to dystrophin)	2.5	1.4
214643_x_at	BIN1	Bridging integrator 1	2.5	1.1
201079_at	SYNGR2	Synaptogyrin 2	2.5	0.7
222022_at	DTX3	Deltex 3 homolog (Drosophila)	2.5	1.2
215222_x_at		Microtubule-actin crosslinking factor 1	2.4	0.8
210201_x_at	BIN1	Bridging integrator 1	2.3	0.9
207968_s_at	MEF2C	MADS box transcription enhancer factor 2, polypeptide C (myocyte enhancer factor 2C)	2.3	1.0

Table 2 (continued)

Gene name	Common	Description	Rh4 fold change upregulation si versus sc	RD fold change upregulation si versus sc
209926_at	MEF2B	MADS box transcription enhancer factor 2, polypeptide B (myocyte enhancer factor 2B)	2.2	1.1
209200_at	MEF2C	MADS box transcription enhancer factor 2, polypeptide C (myocyte enhancer factor 2C)	2.2	1.0
219107_at	BCAN	Brevican	2.2	1.1
216887_s_at	LDB3	LIM domain binding 3	2.2	1.0
210360_s_at	MTSS1	Metastasis suppressor 1	2.1	0.7
206813_at	CTF1	Cardiotrophin 1	2.1	0.8
202222_s_at	DES	Desmin	2.1	0.7
203004_s_at	MEF2D	MADS box transcription enhancer factor 2, polypeptide D (myocyte enhancer factor 2D)	2.1	0.8
201792_at	AEBP1	AE-binding protein 1	2.0	0.9

expression, and promoter studies identified two paired domain binding sites in the TFAP2B promoter.

Further supporting the notion that TFAP2B is a physiologically relevant *in vivo* target gene comes from the recent observation that TFAP2B is a highly specific and sensitive marker for translocation-positive aRMS in immunohistochemical analysis (Wachtel *et al.*, 2006). This study directly confirms *in vivo* expression of the TFAP2B protein in a large number of tumor samples. Importantly, a similar behavior was observed for CDH3 (p-cadherin), and also this gene was identified in our study. Therefore, it very likely represents an additional *in vivo* target gene of PAX3/FKHR.

Next, the physiological relevance of TFAP2B for aRMS cell growth and survival was directly examined. Our data showed that downregulation of TFAP2B in aRMS cells induced apoptosis as efficiently as downregulation of PAX3/FKHR. Interestingly, induction of apoptosis by silencing of PAX3/FKHR could be prevented by TFAP2B overexpression. These results suggest that TFAP2B is directly involved in transduction of a PAX3/FKHR regulated oncogenic characteristic namely anti-apoptotic properties. Identification and analysis of the downstream apoptotic mechanisms is currently ongoing and may identify additional therapeutic target genes. In addition, these rescue experiments directly demonstrate that our target gene signature is not due to any off-target effects of siRNA treatment.

In conclusion, we identified a comprehensive signature of *in vivo* PAX3/FKHR target genes, which are likely involved in mediating several oncogenic properties of the fusion protein such as migration, differentiation and survival. Indeed, TFAP2B mediates, at least in part, the survival function of PAX3/FKHR. Our approach of silencing fusion genes in its cellular context combined with *in vivo* expression data appears to be highly successful for identification of physiological targets to develop new therapeutics.

Materials and methods

Cell lines and plasmids

Rh4 aRMS cells were kindly provided by Peter Houghton (St Jude Children's Research Hospital, Memphis, TN, USA). RD

eRMS and 293T human embryonic kidney cells were obtained from ATCC (LGC Promochem, Molsheim Cedex, France).

The PAX3/FKHR construct consists of 3.7 kb insert cloned into pcDNA3 vector, PAX3/FKHR-derived mutants have a single-point mutation G48S or N269A located in the paired and homeodomain, respectively.

For generation of Rh4 cells stably overexpressing murine TFAP2B, cells were transfected with the pcDNA3.1Neo plasmid containing a 1.8 kb TFAP2B insert. Mock transfection with pcDNA3.1Neo was performed in parallel as control. Selection of stably transfected cells was performed with 1 mg/ml G-418 sulfate (Promega, Wallisellen, Switzerland).

siRNA-mediated silencing

PAX3 and PAX3/FKHR knockdown was induced by RNAi (Elbashir *et al.*, 2001). A total of 2×10^5 Rh4 or RD cells was plated and 24 h later transfected with a combination of two chemically synthesized siRNAs (5'-AAGAGAGAACCCGGGCAUG-dTdT and 5'-CAUGGAUUUCCAGCUAUA-dTdT) both targeting the PAX3 part of the fusion gene (Qiagen, Hombrechtikon, Switzerland). For downregulation of TFAP2B, Rh4 cells were transfected with siRNA with the sequence 5'-ACUUCGAAGUACAAAGUAA-dTdT (Qiagen, catalog no. S100049259). As positive control siRNA targeting glyceraldehyde-3-phosphate dehydrogenase (GAPDH) (catalog no. 4605, Ambion, Huntingdon, UK) was used, as negative control siRNA with the sequence 5'-UUCUUCGAACGUGU CACGU-dTdT (Qiagen, catalog no. 1022076) with no known homology to mammalian genes. Transfection was carried out according to the manufacturer's instructions using 7 μ l of GeneEraser (Stratagene, La Jolla, CA, USA) and 20 nM siRNA (final concentration).

Quantitative RT-PCR

Total RNA (1 μ g) was reverse transcribed with Oligo(dT)₁₅ Primer using the Omniscript Reverse Transcription Kit (Qiagen). qRT-PCR detection of PAX3, TFAP2B and GAPDH was carried out with the commercially available assays-on-demand Hs00240950_m1, Hs00231468_m1 and Hs99999905_m1 (Applied Biosystems, Rotkreuz, Switzerland), respectively. qRT-PCR detection of PAX3/FKHR was performed using PAX3 For (5'-GCACTGTACACCAAGCAGC-3') and FKHR Rev (5'-AACTGTGATCCAGGGCTGTC-3') primers applying the fluorescent SYBR green method (Applied Biosystems) on an Applied Biosystems 7900HT.

Western blot

About 10 μ g of nuclear protein was used for western blotting using NuPAGE electrophoresis system (Invitrogen, Basel,

Switzerland). For PAX3 detection a goat-anti-PAX3 antibody (Santa Cruz Biotechnology, Heidelberg, Germany), for PAX3/FKHR detection a rabbit-anti-FKHR antibody (Cell Signaling Technology, Allschwil, Switzerland) and for detection of TFAP2B protein, a mouse-anti-TFAP2B antibody (Abcam, Cambridge, UK) were used.

Gene expression analysis

Global changes in gene expression were measured using Affymetrix HGU-133A GeneChip arrays (Affymetrix Inc., Santa Clara, CA, USA). cRNA target synthesis and experimental procedures for GeneChip hybridization and scanning were carried out according to the 'GeneChip eukaryotic small sample target labeling technical note' (Affymetrix). Expression data of siRNA, scRNA (control) and non-treated cells was analysed using dChip2004 (Li and Wong, 2001) and GeneSpring7.0 with default normalization and a cross-gene-error model, resulting in 16221 genes. Representative data from two biological replicates are shown.

Cell proliferation assays

Cell proliferation was measured using the 3-(4,5-dimethylthiazol-2-yl)-2,5-diphenyltetrazolium bromide (MTT) assay (Roche, Rotkreuz, Switzerland). Before MTT measurement, a standard curve for each cell line was generated using 500 to 1×10^5 cells per well. A total of 1×10^4 Rh4 or RD cells were plated per 96-well and transfected 24 h later. The amount of converted MTT reagent was measured at different time points up to 72 h later by a multi-detection microplate reader (Bio-Tek Instruments Inc., Littau, Switzerland).

Apoptosis assays

One thousand cells from each experimental condition were assayed for caspase-3 activation using the caspase-Glo 3/7 Assay (Promega, Wallisellen, Switzerland) according to the manufacturer's instructions. Caspase activity was measured at an excitation wavelength of 485 nm and an emission wavelength of 516 nm. For the calculation of standard deviations, first the quotient of treated versus untreated cells was determined. The s.d. of the quotient was then calculated as follows: for two numbers, A and B, with standard deviations, a and b, $(A \pm a)/(B \pm b) = (C \pm c)$ and $c = A/B * \sqrt{((a/A)^2 + (b/B)^2)}$.

For fluorescence-activated cell scanning (FACS) analysis, Rh4 cells from one confluent 35 mm dish were stained with 200 μ l of propidium iodide (PI) followed by cytometry analysis on a Cytomics FC500 Instrument (Beckman Coulter, Nyon, Switzerland). The flow cytometry data were then analysed by the FlowJo software.

Cloning of the TFAP2B promoter and generation of deletion constructs

TFAP2B promoter region from positions -3200 to +1 was amplified by PCR (primer: For, 5'-AAAGTACGAGTGTAACTACTCTGG-3'; Rev, 5'-GCAGCCTGGTCTCTAGGAGG-3') from 293T cell genomic DNA and cloned into the pGL3 basic luciferase vector (Promega, Wallisellen, Switzerland). Deletion constructs were prepared using the Erase-a-base Kit (Promega), allowing progressive unidirectional deletions of approximately 200 bp at the 5' end of the insert.

References

Anderson J, Ramsay A, Gould S, Pritchard-Jones K. (2001). PAX3-FKHR induces morphological change and enhances

Luciferase assay

A total of 1×10^5 293T cells were plated per 35 mm plate and cotransfected 24 h later with 2 μ g of TFAP2B promoter in pGL3basic plasmid plus 1 μ g of either PAX3/FKHR or PAX3/FKHR-derived mutants or pcDNA empty vector plus 100 ng of pFIV-CMV-LacZ control plasmid (System Biosciences, Heidelberg, Germany) using the Ca_2PO_4 transfection method. After 24 h cells were lysed in reporter lysis buffer and assayed for luciferase as well as β -galactosidase activity using the corresponding assay systems (Promega). Luciferase activity values were normalized to the β -galactosidase activity and expressed as relative luciferase units.

ChIP assay

ChIP was performed using a commercially available ChIP-IT enzymatic kit (Active Motif, Rixensart, Belgium) according to manufacturer's instructions. 293T cells were cotransfected with two different deletion constructs, TFAP2B_1 or TFAP2B_2 containing 1592 and 806 bp of the TFAP2B upstream promoter region, respectively and a PAX3 construct encoding for His-tagged PAX3 protein. DNA-bound protein was immunoprecipitated using an anti-His (Qiagen) antibody or mouse IgG (Active Motif) as negative control. For quantification of coprecipitated DNA, amplification of a 470 bp region of the TFAP2B promoter with primer: For, 5'-GCGCAGA GATCCTCTTCTGG-3'; and Rev, 5'-AGCAACGTACGCA CACGTTTC-3' was measured by SYBR Green qRT-PCR. Signals of the anti-His precipitates were normalized to the signals of the IgG precipitates.

Electrophoretic mobility shift assays

Electrophoretic mobility shift assays were performed using the Chemiluminescent Nucleic Acid Detection Module (Pierce, Rockford, IL, USA) according to manufacturer's instructions. Each protein-DNA binding reaction was carried out using 8 μ l of nuclear extracts from PAX3-His or PAX3/FKHR transiently transfected 293T cells and 20 fmol of biotin-labeled double-stranded oligonucleotides corresponding to two possible PAX3-binding sites. Deletion site2-specific sequences Del2 (5'-AGATCCTCTTCTGGGCGTCTGTTCGGGCTATGAG AAGCTCTCCGCA-3') and as control Del2Contr (5'-AGAT CCTCTTCTGGGCGTCTAAAAAAGCTATGAGAAGCTC TCCGCA-3') as well as deletion site3-specific sequences Del3 (5'-GGGGATGGGAAAGGGGGAACAGGGGAACAGAT GAGTATTCATTTC-3') and the control Del3Contr (5'-GG GGTGGGAAAGGGAAAAAAGAAAAAGATGAGT ATTCATTTC-3') were synthesized as 5'-biotin-labeled complementary oligonucleotide pairs (Microsynth, Balgach, Switzerland).

Acknowledgements

We thank FG Barr (University of Pennsylvania, Philadelphia, PA) and R Fässler (Max-Planck-Institute, Munich, Germany) for providing cDNA constructs, A Patrignani (FGCZ) for excellent technical assistance with Affymetrix experiments and M Dettling for performing principal component analysis. This work was supported by Swiss National Science Foundation, grant nos. 3100-067841 and 3100-109837 and the Schweizerische Forschungsförderung Kind und Krebs.

cellular proliferation and invasion in rhabdomyosarcoma. *Am J Pathol* **159**: 1089-1096.

- Ayyanathan K, Fredericks WJ, Berking C, Herlyn M, Balakrishnan C, Gunther E *et al.* (2000). Hormone-dependent tumor regression *in vivo* by an inducible transcriptional repressor directed at the PAX3-FKHR oncogene. *Cancer Res* **60**: 5803–5814.
- Begum S, Emani N, Cheung A, Wilkins O, Der S, Hamel PA. (2005). Cell-type-specific regulation of distinct sets of gene targets by Pax3 and PAX3/FKHR. *Oncogene* **24**: 1860–1872.
- Bennicelli JL, Fredericks WJ, Wilson RB, Rauscher III FJ, Barr FG. (1995). Wild type PAX3 protein and the PAX3-FKHR fusion protein of alveolar rhabdomyosarcoma contain potent, structurally distinct transcriptional activation domains. *Oncogene* **11**: 119–130.
- Bernasconi M, Remppis A, Fredericks WJ, Rauscher III FJ, Schafer BW. (1996). Induction of apoptosis in rhabdomyosarcoma cells through down-regulation of PAX proteins. *Proc Natl Acad Sci USA* **93**: 13164–13169.
- Davicioni E, Finckenstein FG, Shahbazian V, Buckley JD, Triche TJ, Anderson MJ. (2006). Identification of a PAX-FKHR gene expression signature that defines molecular classes and determines the prognosis of alveolar rhabdomyosarcomas. *Cancer Res* **66**: 6936–6946.
- Edelman GM, Jones FS. (1995). Developmental control of N-CAM expression by Hox and Pax gene products. *Philos Trans R Soc London B Biol Sci* **349**: 305–312.
- Elbashir SM, Lendeckel W, Tuschl T. (2001). RNA interference is mediated by 21- and 22-nucleotide RNAs. *Genes Dev* **15**: 188–200.
- Epstein JA, Shapiro DN, Cheng J, Lam PY, Maas RL. (1996). Pax3 modulates expression of the c-Met receptor during limb muscle development. *Proc Natl Acad Sci USA* **93**: 4213–4218.
- Epstein JA, Song B, Lakkis M, Wang C. (1998). Tumor-specific PAX3-FKHR transcription factor, but not PAX3, activates the platelet-derived growth factor alpha receptor. *Mol Cell Biol* **18**: 4118–4130.
- Fredericks WJ, Galili N, Mukhopadhyay S, Rovera G, Bennicelli J, Barr FG *et al.* (1995). The PAX3-FKHR fusion protein created by the t(2;13) translocation in alveolar rhabdomyosarcomas is a more potent transcriptional activator than PAX3. *Mol Cell Biol* **15**: 1522–1535.
- Galili N, Davis RJ, Fredericks WJ, Mukhopadhyay S, Rauscher III FJ, Emanuel BS *et al.* (1993). Fusion of a fork head domain gene to PAX3 in the solid tumour alveolar rhabdomyosarcoma. *Nat Genet* **5**: 230–235.
- Ginsberg JP, Davis RJ, Bennicelli JL, Nauta LE, Barr FG. (1998). Up-regulation of MET but not neural cell adhesion molecule expression by the PAX3-FKHR fusion protein in alveolar rhabdomyosarcoma. *Cancer Res* **58**: 3542–3546.
- Keller C, Arenkiel BR, Coffin CM, El-Bardeesy N, DePinho RA, Capecchi MR. (2004). Alveolar rhabdomyosarcomas in conditional Pax3:Fkhr mice: cooperativity of Ink4a/ARF and Trp53 loss of function. *Genes Dev* **18**: 2614–2626.
- Khan J, Simon R, Bittner M, Chen Y, Leighton SB, Pohida T *et al.* (1998). Gene expression profiling of alveolar rhabdomyosarcoma with cDNA microarrays. *Cancer Res* **58**: 5009–5013.
- Lam PY, Sublett JE, Hollenbach AD, Roussel MF. (1999). The oncogenic potential of the Pax3-FKHR fusion protein requires the Pax3 homeodomain recognition helix but not the Pax3 paired-box DNA binding domain. *Mol Cell Biol* **19**: 594–601.
- Lang D, Lu MM, Huang L, Engleka KA, Zhang M, Chu EY *et al.* (2005). Pax3 functions at a nodal point in melanocyte stem cell differentiation. *Nature* **433**: 884–887.
- Li C, Wong WH. (2001). Model-based analysis of oligonucleotide arrays: expression index computation and outlier detection. *Proc Natl Acad Sci USA* **98**: 31–36.
- Margue CM, Bernasconi M, Barr FG, Schafer BW. (2000). Transcriptional modulation of the anti-apoptotic protein BCL-XL by the paired box transcription factors PAX3 and PAX3/FKHR. *Oncogene* **19**: 2921–2929.
- Mayanil CS, George D, Freilich L, Miljan EJ, Mania-Farnell B, McLone DG *et al.* (2001). Microarray analysis detects novel Pax3 downstream target genes. *J Biol Chem* **276**: 49299–49309.
- Moser M, Dahmen S, Kluge R, Grone H, Dahmen J, Kunz D *et al.* (2003). Terminal renal failure in mice lacking transcription factor AP-2 beta. *Lab Invest* **83**: 571–578.
- Moser M, Pscherer A, Roth C, Becker J, Mucher G, Zerres K *et al.* (1997). Enhanced apoptotic cell death of renal epithelial cells in mice lacking transcription factor AP-2beta. *Genes Dev* **11**: 1938–1948.
- Scheidler S, Fredericks WJ, Rauscher III FJ, Barr FG, Vogt PK. (1996). The hybrid PAX3-FKHR fusion protein of alveolar rhabdomyosarcoma transforms fibroblasts in culture. *Proc Natl Acad Sci USA* **93**: 9805–9809.
- Tomescu O, Xia SJ, Strezlecki D, Bennicelli JL, Ginsberg J, Pawel B *et al.* (2004). Inducible short-term and stable long-term cell culture systems reveal that the PAX3-FKHR fusion oncoprotein regulates CXCR4, PAX3, and PAX7 expression. *Lab Invest* **84**: 1060–1070.
- Wachtel M, Dettling M, Koscielniak E, Stegmaier S, Treuner J, Simon-Klingenstein K *et al.* (2004). Gene expression signatures identify rhabdomyosarcoma subtypes and detect a novel t(2;2)(q35;p23) translocation fusing PAX3 to NCOA1. *Cancer Res* **64**: 5539–5545.
- Wachtel M, Runge T, Leuschner I, Stegmaier S, Koscielniak E, Treuner J *et al.* (2006). Subtype and prognostic classification of rhabdomyosarcoma by immunohistochemistry. *J Clin Oncol* **24**: 816–822.
- Xia SJ, Barr FG. (2004). Analysis of the transforming and growth suppressive activities of the PAX3-FKHR oncoprotein. *Oncogene* **23**: 6864–6871.
- Zhang L, Wang C. (2006). Identification of a new class of PAX3-FKHR target promoters: a role of the Pax3 paired box DNA binding domain. *Oncogene* **26**: 1595–1605.

Supplementary Information accompanies the paper on the Oncogene website (<http://www.nature.com/onc>).